# Semibatch Aqueous-Solution Polymerization of Acrylic Acid: Simultaneous Control of Molar Masses and Reaction Temperature

Roque J. Minari, Gerardo Caceres, Paola Mandelli, Mariana M. Yossen, Manuel Gonzalez-Sierra, Jorge R. Vega, Luis M. Gugliotta*

The semibatch polymerization of non-ionized acrylic acid (AA) was investigated with the aim of producing poly(acrylic acid) (PAA) of controlled molar masses, at complete AA conversion, and under safe conditions. The proposed strategy mainly consists in feeding the AA at a constant rate along the reaction, for simultaneously controlling polymerization rate and molar masses. PAA of intermediate $\overline{M}_n$, in the range $1 \times 10^4$–$2 \times 10^5$ g · mol$^{-1}$, was produced through an adequate selection of both the initiator concentration and the AA flow rate. In all experimental conditions, backbiting reactions were confirmed by $^{13}$C NMR. A simple mathematical model was developed to help interpret the experimental results.

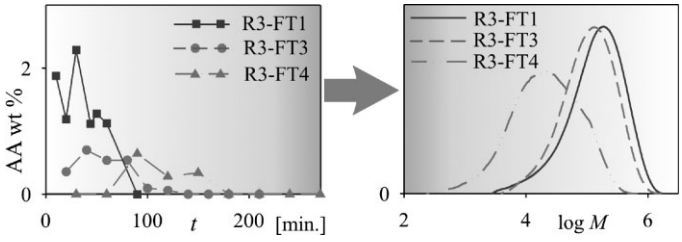


## Introduction

Water-soluble polymers containing acrylic acid (AA), or their metallic salts, are useful in a wide range of applications including super-absorbents materials, paints, membranes, ceramics, textiles, biomaterials, flocculants, thickeners, sludge dispersants, ion-exchange resins, and sedimentation products.[1,2] Applications of AA-based polymers depend on their molar mass distribution (MMD) and degree of ionization. For instance, neutralized salts of poly(acrylic acid) (PAA) having low molar masses are used as sludge dispersants;[3] while some high molar mass PAAs are employed as thickener and flocculating agents.

AA is mainly polymerized in aqueous solutions. Due to the high AA reactivity, two main problems arise when PAA is obtained through batch processes: (i) high polymerization rates and consequently huge heat generations to be removed in short time periods, which preclude a safe process operation; and (ii) the final product exhibits extremely large molar masses. Thus, the synthesis of PAA under safe conditions and with controlled molar masses requires the design of special control policies aimed at avoiding large AA concentrations [AA], which would lead to extremely high polymerization rates and reaction heat.[4]

Polymers of AA presenting low molar masses have been synthesized in aqueous solution at temperatures of 50–100 °C, by employing low monomer concentrations (15–30 wt.-%), water-soluble initiators, and chain transfer agents (CTA).[4] More effective synthesis methods often employ redox initiators (ammonium persulfate: APS/alkali metal/alkali metal pyrosulfite), and different CTAs (e.g., acetic acid, isopropanol and mercaptoethanol).[4,5]

R. J. Minari, G. Caceres, P. Mandelli, M. M. Yossen, J. R. Vega, L. M. Gugliotta
INTEC, Universidad Nacional del Litoral-CONICET, Güemes 3450, 3000 Santa Fe, Argentina
Fax: (+54) 342 4511079; E-mail: lgug@intec.unl.edu.ar
M. Gonzalez-Sierra
IQUIR, Universidad Nacional de Rosario-CONICET, Suipacha 531, 2000 Rosario, Argentina
J. R. Vega
Facultad Regional Santa Fe, Universidad Tecnológica Nacional, Lavaisse 610, 3000 Santa Fe, Argentina




DOI: 10.1002/mren.201000059

Bokias et al.[6] investigated the control of the average molar masses of PAA produced in batch aqueous-solution polymerization at low solids content and moderate temperature (35 °C), by varying the persulfate/sodium metabisulfite ratio of the redox initiation system. The main disadvantage of such strategy was the high amount of couple redox required for producing PAA of low molar masses. Several publications on aqueous-solution AA polymerization aim at determining the reaction conditions for synthesizing highly branched PAA used in the production of super-absorbent polymers. For example, Omidian et al.[7] investigated the influence of reaction temperature, KPS concentration ([KPS]), and $O_2$ inhibition on the PAA absorbance capability.

Concerning the production of water soluble polymers, relatively few publications have dealt with kinetic mechanisms, mathematical models, and control operation strategies. For the synthesis of PAA, Anseth et al.[8] and Çatalgil-Giz et al.[9] investigated the influence of the AA ionization degree, the pH, and the solution ionic strength on both the polymerization rate and the average molar masses. The pulsed-laser polymerization (PLP) of AA at low temperature (between 6 and 20 °C) in combination with size exclusion chromatography (SEC) have been applied for investigating the influence of the AA and PAA concentrations, and the occurrence of backbiting reactions on the AA propagation-rate coefficient.[10,11] For the aqueous-phase polymerization of methacrylic acid carried out under batch conditions, the dependence of propagation, and termination rate coefficients on monomer concentration and conversion was also taken into account, as a part of kinetics and mathematical modeling studies.[12,13]

In this work, the isothermal aqueous-solution polymerization of AA carried out under semibatch conditions are investigated with the aim of producing PAA of controlled molar masses and low content of free AA. The proposed control strategy simultaneously produces a tight regulation of the reaction temperature, and therefore allows a safe process operation that would enable its implementation at industrial scale. Also, some kinetic aspects of the aqueous AA polymerization are assessed, and a simple mathematical model is developed for a better interpretation of the experimental data.

## Experimental Section

### Materials

Technical grade AA inhibited with hydroquinone monomethylether (Kimiker S.R.L., Argentina), was used without previous purification. KPS (Anedra, 99% purity) was used as initiator. Hydroquinone (Fluka AG, >99% purity) was employed as polymerization inhibitor. A set of six linear Pullulan standards (*Shodex Standards* P-82) was used for determining the molar mass calibration of the chromatographic system. The following reagents were used to prepare the eluent for SEC: $NaH_2PO_4$, $Na_2HPO_4$, and $NaNO_3$ (all from Cicarelli Argentina, >98% purity). Distilled and deionized water was used throughout the work.

### Polymerizations

Semibatch aqueous-solution polymerizations were carried out in a 1 L jacketed glass reactor equipped with an automatic feeding system, a digital thermometer, a reflux condenser, a stirrer, a sampling device, and a nitrogen inlet. The set point for the reaction temperature ($T_r$) was $T_r^d = 60$ °C; and $T_r$ was indirectly regulated by controlling the water temperature in the reactor jacket through a thermostatic bath.

For different [KPS] and feeding times (FT), several polymerizations were carried out as follows. Initially, water and KPS were loaded into the reactor. After reaching $T_r \cong 60$ °C, an aqueous solution of AA was fed at a constant flow rate and ambient temperature. After the feeding period, the reaction was continued in batch along 30 min. Then, the inhibitor was added to stop the reaction. During polymerizations, $N_2$ was continuously bubbled at a flow rate of 50 $cm^3 \cdot min^{-1}$.

Ten experiments were carried out (see Table 1) employing recipes of 20% solids content. Experiments indicated as R1- to R4- were carried out at four different [KPS] (0.75, 2.30, 3.00, and 6.00% weight based on monomer; wbm). For experiments R1- and R3- (of low and intermediate [KPS]), the following AA FT were employed: FT1 = 60 min, FT2 = 120 min, FT3 = 180 min, and FT4 = 240 min.

### Sampling and Characterization

Samples were withdrawn along the polymerizations for measuring the total and fractional monomer conversions ($x$ and $x_f$, respectively), and the MMD and their number- and weight-averages ($\overline{M}_n$ and $\overline{M}_w$). The final product of each polymerization

*Table 1.* Semibatch polymerizations of AA. Employed [KPS] and AA FT (solids content = 20% and $T_r^d = 60$ °C).

| Experiment[a)] | [KPS] [% wbm] | AA FT [min] |
|---|---|---|
| R1-FT1 | 0.75 | 60 |
| R1-FT2 | 0.75 | 120 |
| R1-FT3 | 0.75 | 180 |
| R1-FT4 | 0.75 | 240 |
| R2-FT2 | 2.30 | 120 |
| R3-FT1 | 3.00 | 60 |
| R3-FT2 | 3.00 | 120 |
| R3-FT3 | 3.00 | 180 |
| R3-FT4 | 3.00 | 240 |
| R4-FT2 | 6.00 | 120 |

[a)]The number next to the label "FT" indicates the AA feeding period (in h).

was also characterized by $^{13}C$ and H NMR for elucidating, from the analysis of the molecular structure, main reactions involved in the kinetic mechanism, as well as for quantifying the branching degree (BD). A relatively high sampling time (between 10 and 30 min) was selected as a reasonable trade-off between an acceptable monitoring along the semicontinuous reaction and a reduce disturbance in the total reactant masses.

Monomer conversions were gravimetrically measured after drying the samples until constant weight (at 60 °C). The MMD was determined by SEC. The chromatographic system involved a Waters 1515 isocratic pump, fitted with a set of 5 Ultrahydrogel columns of nominal fractionation range $5 \times 10^3$–$7 \times 10^6$ g · mol$^{-1}$, and a Waters 2414 differential refractometer (DR). The following aqueous buffer solution was used as eluent: $NaH_2PO_4/NaHPO_4$ $50 \times 10^{-3}$ M (pH = 7) + $NaNO_3$ $50 \times 10^{-3}$ M, at a flow rate of 0.8 mL · min$^{-1}$. An injection loop of 200 μL was used. Samples for SEC were prepared from liquid PAA directly taken from the reactor and diluted in the eluent buffer at a concentration of around 5 mg · mL$^{-1}$. These relatively high concentrations were selected to improve the signal-to-noise ratio and the baseline definition at high elution volumes, where the solvent peaks can strongly distort the sample chromatograms. The measured signals were treated through an ad hoc data processing software that was specially developed to compensate for artifacts introduced by the column overloading due to the required high-concentration injections (i.e., spurious column elution-volume shifts and additional broadening).[14] The MMD was estimated by combining the corrected DR chromatograms with the molar mass calibration determined on the basis of narrow pullulan standards, in the range $5 \times 10^4$–$8 \times 10^5$ g · mol$^{-1}$. Thus, all molar masses reported in this work are referred to pullulans.

The variable BD herein used is defined as the percentage of number of branches with respect to the number of bound monomer units, and it is calculated as:

$$\mathrm{BD}\,(\%) = \frac{A(\mathrm{Cq})}{A(\mathrm{C=O})} \times 100 \qquad (1)$$

where $A$(Cq) and $A$(C=O) are the areas of the branched quaternary site and the bound carbonyl carbon, respectively; both determined from the $^{13}C$ NMR spectra. The $^{13}C$ chemical shifts for these carbons are centered at 47.6 and 172–180 ppm for the Cq and the C=O sites, respectively, as indicated in Figure 1. NMR characterizations were carried out in a Bruker Avance 300 spectrometer (operating at 300.14 MHz in $^1H$ and 75.14 MHz in $^{13}C$). To this effect, several PAA liquid samples (0.4 mL) containing $D_2O$ (0.05–0.1 mL) in a 5 mm NMR tube were measured. For a complete structural analysis, a series of 1D and 2D NMR spectra, including $^1H$, $^{13}C$, HSQC-Dept-edited, HH Cosy, and HMBC using the Bruker standard software were performed. For the proton spectra, the 1D sequence using water suppression with f1 presaturation was used. A 1D sequence with power-gated decoupling fast-phasegel experiment (30° flip angle; Ad: 75 ms; d1: 0.1 s, measuring time typically 120 000–150 000 scans, corresponding to 5–8 h) was used for the $^{13}C$ measurements and allowed us the determination of the Cq amount.[15] Besides the main chain polymer, several smaller molecules (3-hydroxy propionic acid, hydroquinone, and

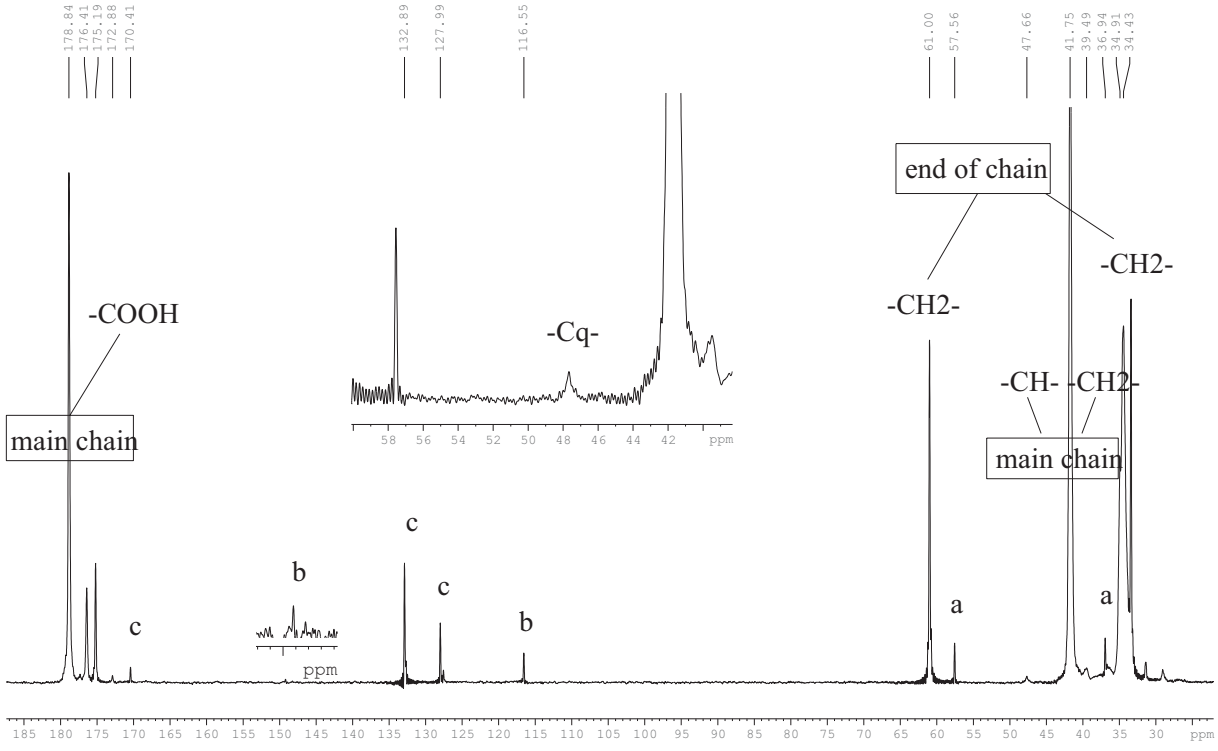


*Figure 1.* $^{13}C$ NMR spectrum of the PAA obtained at the end of experiment R1-FT3. Peaks a, b, and c correspond to 3-hydroxy propionic acid, hydroquinone, and unreacted AA, respectively.

*Table 2.* Semibatch polymerizations with AA FT = 120 min. Experimental values of final conversions, average molar masses, and BDs, for several [KPS].

| Experiment | $x$ [%] | $\overline{M}_n$ [g · mol$^{-1}$] | $\overline{M}_w$ [g · mol$^{-1}$] | BD |
|---|---|---|---|---|
| R1-FT2 | 99.2 | 166 000 | 531 000 | 2.1 |
| R2-FT2 | 100 | 132 000 | 340 000 | – |
| R3-FT2 | 100 | 73 000 | 213 000 | 4.3 |
| R4-FT2 | 100 | 56 000 | 144 000 | – |

unreacted AA) were found and easily singled out by means of a DOSY experiment. The peaks of such small molecules are, respectively, indicated by (a), (b), and (c) in the spectrum of Figure 1.

## Results and Discussion

In what follows, the effect of different initial [KPS] in the recipe as well as the modification of the feeding period on the evolution and final values of several polymerization variables is analyzed.

### Effect of the Initial [KPS]

The effect of the initial [KPS] was analyzed by adopting an AA FT of 120 min (experiments R1-FT2, R2-FT2, R3-FT2, and R4-FT2). Table 2 summarizes the final values of $x$, $\overline{M}_n$, $\overline{M}_w$, and BD; and Figure 2 shows the experimental evolution of

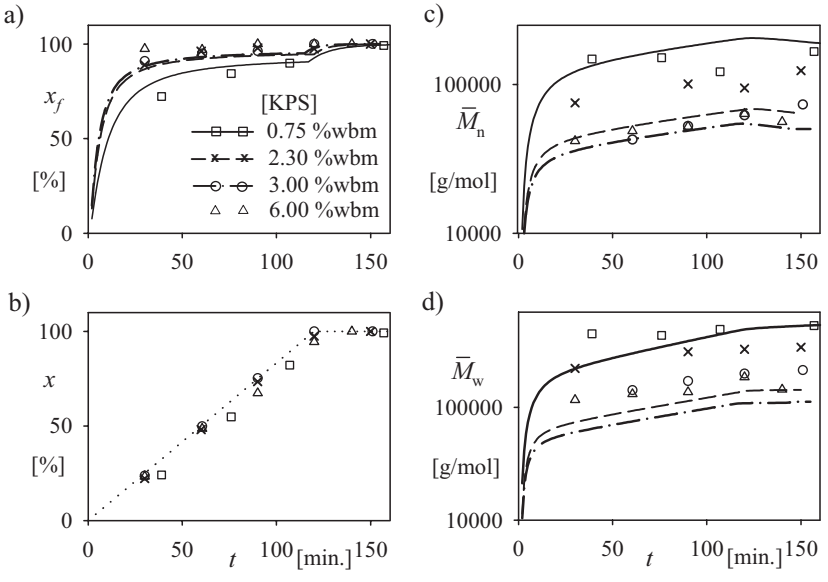


*Figure 2.* Semibatch polymerizations of AA at several [KPS] for FT = 120 min. Evolution of: (a) fractional conversion, $x_f$; (b) total conversion, $x$; (c,d) number- and weight-average molar masses ($\overline{M}_n$ and $\overline{M}_w$). Experimental results are indicated by symbols and model predictions by traces. The dotted line in Figure 2b indicates the wt.-% of the fed AA.

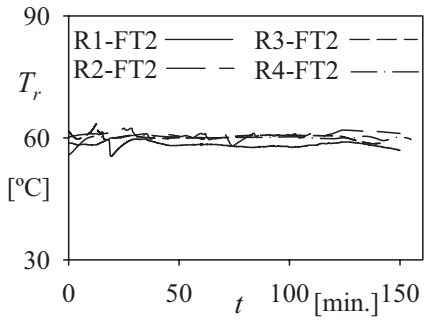


*Figure 3.* Semibatch polymerizations of AA at several [KPS] for FT = 120 min. Evolution of the registered $T_r$ ($T_r^d$ = 60 °C).

$x_f$, $x$, $\overline{M}_n$, and $\overline{M}_w$ (in symbols). In Figure 2b, the dotted line was added to identify the wt.-% of the fed AA. For the four reactions, the registered $T_r$ is represented (in traces) in Figure 3. In all reactions, and in spite of the high AA reactivity, $T_r$ was regulated within the range 60 ± 4 °C.

Except for R1-FT2, complete AA conversions were strictly obtained at the end of reactions (i.e., $x$ = 100% for [KPS] >0.75% wbm). Also, almost complete AA conversions were observed in the course of such reactions [i.e., $x_f(t) > 90\%$ and $x(t)$ close to the wt.-% fed AA line], thus indicating quasi-starved operating conditions (see Figure 2a and b). Notice that the employed AA semicontinuous strategy produced low [AA] in the reaction medium, thus allowing a quite acceptable control of $T_r$ (Figure 3). The small AA accumulation during the polymerization process also guaranties an effective controllability of the reaction heat (i.e., the rate of polymerization is controlled by the monomer addition). This is particularly relevant in industrial applications involving higher reaction volumes.

For FT = 120 min, experimental results indicate that for [KPS] > 0.75% wbm no significant effect is observed on $x$, $x_f$, and $T_r$; however, it strongly affects the average molar masses and BD of the produced PAA. The following is observed: (i) both $\overline{M}_n$ and $\overline{M}_w$ decreased for increasing [KPS] (Table 1 and Figure 2c and d), due to the increment in the radical concentration at a practically fixed monomer concentration; (ii) [KPS] > 3% wbm are required to produce PAA with $\overline{M}_n < 100\,000$ g · mol$^{-1}$; and (iii) molar masses are not significantly reduced for [KPS] > 3% wbm. This last behavior is observed in Figure 2c and d, where small changes are produced on both $\overline{M}_n$ and $\overline{M}_w$ for increments in the [KPS] from 3.0 to 6.0% wbm. Such small effect of [KPS] on molar masses could be attributed to a

*Table 3.* Semibatch polymerizations of AA at several FT and two different [KPS] (0.75 and 3% wbm). Experimental values of final conversions, average molar masses, and BDs.

| Reaction | $x$ [%] | $\overline{M}_n$ [g · mol$^{-1}$] | $\overline{M}_w$ [g · mol$^{-1}$] | BD |
|---|---|---|---|---|
| R1-FT1 | 94.6 | 197 000 | 662 600 | 1.5 |
| R1-FT2 | 99.2 | 166 000 | 531 500 | 2.1 |
| R1-FT3 | 100 | 170 800 | 463 500 | 1.7 |
| R1-FT4 | 100 | 116 500 | 336 500 | 1.8 |
| R3-FT1 | 100 | 68 500 | 217 000 | 2.4 |
| R3-FT2 | 100 | 73 000 | 213 000 | – |
| R3-FT3 | 100 | 61 500 | 160 100 | – |
| R3-FT4 | 100 | 9 000 | 41 500 | 3.2 |

reduction of the initiator effectiveness ($f$) due to the cage effect at high [KPS], which becomes more important at low monomer concentrations.[16] Also noticed that the BD increases with the [KPS] (Table 2), which is in agreement with previous results obtained for the semicontinuous polymerization of butyl acrylate (BA).[17]

### Effect of FT

Consider now the influence of the AA FT on the semibatch polymerization of AA. Table 3 summarizes the final values of $x$, $\overline{M}_n$, and $\overline{M}_w$; and Figures 4 and 5 show the evolutions of $x$, $x_f$, $\overline{M}_n$, and $\overline{M}_w$, for [KPS] = 0.75 and [KPS] = 3% wbm, respectively. For experiments involving low AA FT (FT = 60 min and FT = 120 min.) and the lowest [KPS] (0.75% wbm), the final monomer conversion was lower than 100% (experiments R1-FT1 and R1-FT2, Table 3 and Figures 4a and b). However, for higher [KPS], the AA FT slightly affected the evolution of AA conversions ($x$ and $x_f$), and produced a complete final conversion in all reactions (experiments R3-FT1-4, Table 3 and Figure 5a and b). Furthermore, for [KPS] = 3% wbm and FT > 120 min, starved conditions were almost reached (i.e., $x_f(t) \approx 100\%$). Notice that an adequate selection of the AA FT guaranteed low [AA] in the reaction medium and assured the control of $T_r$ (not shown for space reasons).

Number-average molar masses were practically unaffected by AA FT lower than 180 min. However, with the longest AA FT (=240 min), significant reductions in the average molar masses were observed with respect to those obtained at higher feed rates (Table 3 and Figure 4). At [KPS] = 0.75% wbm, the PAA polydispersity ($\overline{M}_w/\overline{M}_n$) resulted practically unaffected by the AA FT. For increasing FT, a shift of the MMD maximum at lower molar masses ($M$) was observed, without broadening the MMD (Figure 6a). However, for [KPS] = 3.0% wbm and the longest FT (=240 min), increased PAA polydispersity ($\overline{M}_w/\overline{M}_n > 4$) as well as a shoulder at high molar masses were observed (Figure 6b).

Finally, the BD increased with the FT because, at a fixed [KPS], higher FT produced lower [AA], thus increasing the probability of both inter- and intramolecular transfer reactions with respect to propagation reactions.

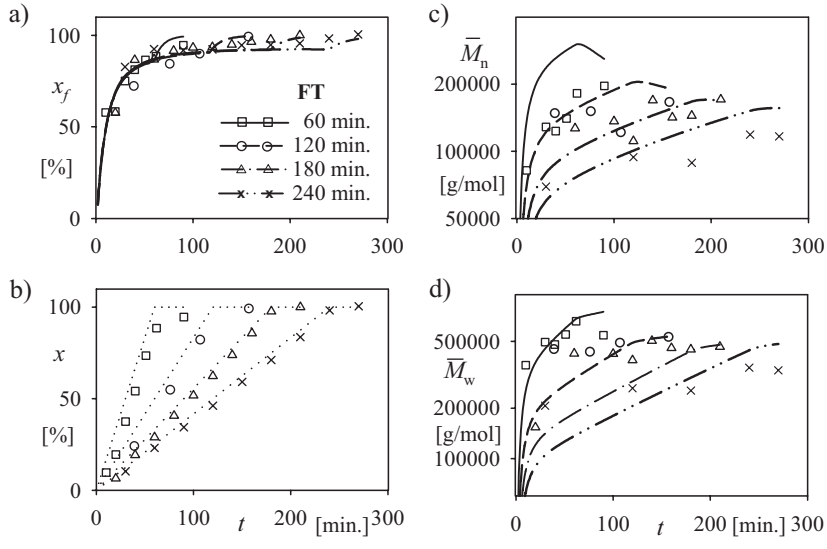


*Figure 4.* Semibatch polymerizations of AA at several FT, for [KPS] = 0.75% wbm. Evolution of: (a) fractional conversion, $x_f$; (b) total conversion, $x$; (c,d) number- and weight-average molar masses ($\overline{M}_n$ and $\overline{M}_w$). Experimental measurements are indicated by symbols and model predictions by traces. (The dotted lines in Figure 4b indicate the wt.-% of the fed AA.)

### Kinetics and Mathematical Model

A simple mathematical model was developed to help interpret the experimental results. It is based on the following kinetic considerations: (i) thermal decomposition of KPS; (ii) generation of a centered-secondary carbon radical, $R^{\bullet}_{sec}(0,0)$, by monomer reaction with sulfate radicals according to Equation (2) [the first and second indexes between brackets in $R^{\bullet}_{sec}(s,l)$ indicate the number of quaternary carbons linked to a short ($s$) branch and to a long ($l$) branch, respectively]; (iii) propagation of $R^{\bullet}_{sec}(s,l)$ with AA according to Equation (3), which allows the polymeric radical growing, not indicated here for simplicity in notation; (iv) bimolecular termination between growing radicals; (v) intermolecular chain transfer to polymer, $P$, by H abstraction from a tertiary C on the PAA according to Equation (4), involving the generation of

a mid-chain centered-tertiary radical, $R^{\bullet}_{tert}(s,l)$, with a new long branching point; (vi) intramolecular H abstraction (backbiting) from a tertiary C on a growing polymeric radical according to Equation (5), involving the generation of a $R^{\bullet}_{tert}(s,l)$ and a new short branch; (vii) propagation of $R^{\bullet}_{tert}(s,l)$ with AA, generating a $R^{\bullet}_{sec}(s,l)$ radical, as it is shown in Equation (6).

$$SO_4^{-\bullet} + AA \rightarrow R^{\bullet}_{sec}(0,0) \quad (2)$$

$$R^{\bullet}_{sec}(s,l) + AA \xrightarrow{k_{p,sec}} R^{\bullet}_{sec}(s,l) \quad (3)$$

$$R^{\bullet}_{sec}(s,l) + \cdots CH_2-(HOOC)CH-CH_2 \cdots \{P\} \xrightarrow{k_{fp}} P + R^{\bullet}_{tert}(s,l+1) \quad (4)$$

$$R^{\bullet}_{sec}(s,l) \xrightarrow{k_{bb}} R^{\bullet}_{tert}(s+1,\ l) \quad (5)$$

$$R^{\bullet}_{tert}(s,l) + AA \xrightarrow{k_{p,tert}} R^{\bullet}_{sec}(s,l) \quad (6)$$

Li and Schork,[18] considered the aqueous-solution polymerization of AA (65% neutralized) at 55 °C. According to these authors, bimolecular termination of AA-radicals could occur by disproportionation, where one saturated dead-polymer chain and one unsaturated dead-polymer chain are formed; and more rarely by combination, when two AA-radicals react to form one saturated dead-polymer molecule.

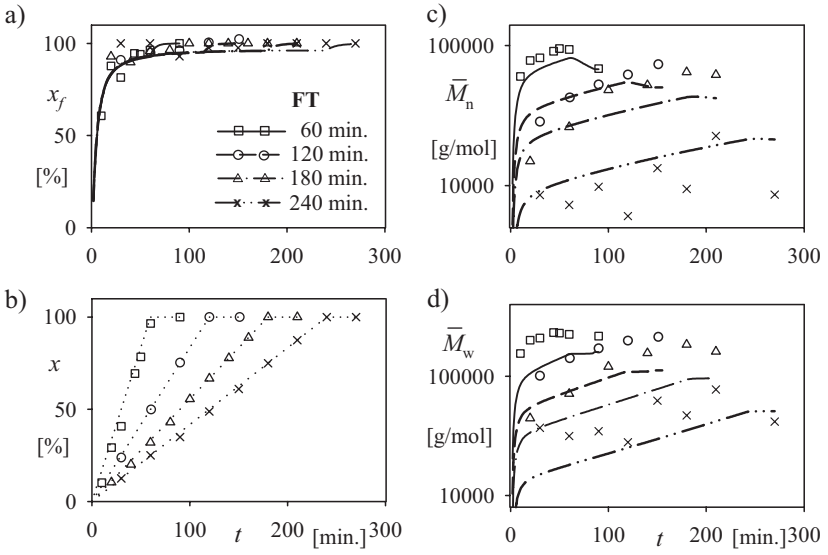


*Figure 5.* Semibatch polymerizations of AA at several FT, for [KPS] = 3% wbm. Evolution of: (a) fractional conversion, $x_f$; (b) total conversion, $x$; (c,d) number- and weight-average molar masses ($\bar{M}_n$ and $\bar{M}_w$). Experimental measurements are indicated by symbols and model predictions by traces. (The dotted lines in Figure 5b indicate the wt.-% of the fed AA.).

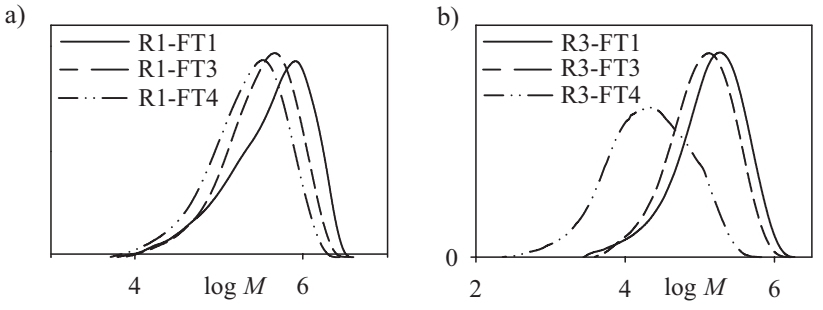


*Figure 6.* Effect of the AA FT on the MMD. (a) [KPS] = 0.75% wbm; (b) [KPS] = 3% wbm. (For increasing FT, the MMD is shifted to lower values of $M$.).

To verify the predominant termination mechanism at the investigated polymerization conditions, $^{13}C$ NMR measurements were used for determining the end chain group (Figure 1). This analysis was also utilized to observe the presence of species generated in Equations (2)–(6). In the olefinic region, other peaks than those of the unreacted monomer were not observed, thus indicating the absence of double bonds at the polymer chain end. On the other hand, the peaks observed at 61 and 34 ppm indicate that the predominant terminal group is a $-CH_2-CH_2OH$. The presence of such end group implies the reaction between the adjacent sulfate and carboxylic groups, which is promoted at high proton concentration and produces the decarboxilation of the attached AA followed by the hydrolysis of the sulfate ester.

These observations demonstrate that the main termination mechanism is by combination, where the chain extremes are identical, and that the amount of polymer produced by both transfer to monomer and termination by disproportionation can be neglected. Our observations are in agreement with the hypothesis of Scott and Peppas,[19] that assumed combination as the main termination mechanism for the batch AA polymerization at 67 °C and at different degrees of neutralization.

The mathematical model considers the following hypothesis: (a) isothermal and dilute solution polymerization conditions; (b) termination by combination and absence of transfer to monomer; (c) AA only consumed by propagation reactions (long-chain hypothesis); (d) generation of $R^{\bullet}_{tert}$ and a new long-chain branch by intermolecular H abstraction from the tertiary C on the chain polymer; (e) generation of $R^{\bullet}_{tert}$ and a new short-chain branch by intramolecular H abstraction from the tertiary C on the propagating radicals; (f) different propagation rate constants for $R^{\bullet}_{sec}$ and $R^{\bullet}_{tert}$; (g) pseudo-stationary states for

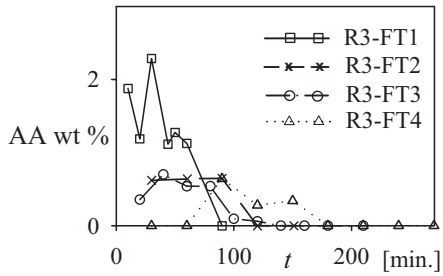


*Figure 7.* Experimental values of free-AA content along the R3-reactions.

all radical species; (h) termination and intra- and intermolecular H abstraction of $R^{\bullet}_{tert}$ negligible; (i) consumption of KPS by acid-catalyzed persulfate decomposition (without producing free radicals) negligible; (j) rate constants not diffusion controlled and independent of the chain length. Hypothesis (f) relies on the reduction in the apparent rate constant of propagation, that was observed by PLP combined with SEC in the aqueous polymerization of AA, where $R^{\bullet}_{tert}$ exhibits a lower reactivity than $R^{\bullet}_{sec}$, as a consequence of backbiting reactions.[11] Main model equations are presented in the Appendix.

Unfortunately, the reported kinetic parameters on the aqueous AA polymerization correspond to: (i) different reaction temperatures to the here adopted;[8,10] or (ii) partially neutralized monomer.[18,20] Lacik et al.[10] reported that the propagation rate constant measured by PLP-SEC depends on the AA concentration. Figure 7 represents the experimental wt.-% of free AA along the R3 reaction set (R3-FT1 to R3-FT4). Notice that when the reaction system is operated under quasi-starved or starved conditions, then the AA concentration remains low and practically constant along the FT, and adopts an almost negligible value after that period. From these observations, and taken into account that the AA concentration remains almost constant along the reaction, it becomes unnecessary to consider a variable propagation rate coefficient. For this reason, it was adopted $k_{p,sec} = 2.79 \times 10^7$ L · mol$^{-1}$ · min$^{-1}$ (at 60 °C), which was estimated from an Arrhenius expression fitted to a temperature interval of 2.8–20.1 °C, for 2 wt.-% of AA.[10]

*Table 4.* Model parameters used for fitting the experimental data ($T_r = 60$ °C).

| | | | |
|---|---|---|---|
| $k_{p,sec}$ [a)] | $2.79 \times 10^7$ L · mol$^{-1}$ · min$^{-1}$ | $k_d$ [b)] | $8.83 \times 10^{-3}$ min$^{-1}$ |
| $k_{p,tert}$ [b)] | $0.71\, k_{p,sec}$ | $k_{fp}$ [b)] | $4.24 \times 10^2$ L · mol$^{-1}$ · min$^{-1}$ |
| $f$ [c)] | 0.5–0.2 [c)] | $k_{bb}$ [b)] | $7.93 \times 10^4$ min$^{-1}$ |
| $k_{tc}$ [b)] | $8.91 \times 10^{11}$ L · mol$^{-1}$ · min$^{-1}$ | | |

[a)]Estimated from an Arrhenius expression;[10] [b)]Adjusted in this work from reactions R1-, R2-, and R3-; [c)]For reactions R1-, R2-, and R3- the adopted value was $f = 0.5$, and for R4 it was adjusted to $f = 0.2$.

To fit the experimental data of $x$, $\overline{M}_n$, $\overline{M}_w$, and BD for reactions R1-, R2-, and R3-, the following rate constants were adjusted: (i) propagation to tertiary radicals ($k_{p,tert}$), (ii) termination by combination ($k_{tc}$), (iii) initiator decomposition ($k_d$) at the reaction conditions, and (iv) inter- and intramolecular chain transfer to polymer ($k_{fp}$, $k_{bb}$, respectively). To this effect, the normalized absolute error between experimental and simulated values was minimized by employing a genetic algorithm-based optimization routine.

The employed model parameters are summarized in Table 4 and the simulation results are represented by traces in Figures 2, 4, and 5. For the final products of each reaction, Table 5 compares the model predictions of BD, and its contributions $BD_s$ and $BD_l$, with the experimental values. According to simulation results, PAA exhibits short

*Table 5.* Comparison between experimental and simulated BDs.

| Experiment | $^{13}$C NMR measurement | Simulation results | | |
|---|---|---|---|---|
| | BD [%] | BD [%] | $BD_s$ [%] | $BD_l$ [%] |
| R1-FT1 | 1.5 | 1.02 | 1.01 | $8.90 \times 10^{-3}$ |
| R1-FT2 | 2.1 | 1.56 | 1.55 | $1.26 \times 10^{-2}$ |
| R1-FT3 | 1.7 | 1.84 | 1.83 | $1.39 \times 10^{-2}$ |
| R1-FT4 | 1.8 | 2.13 | 2.12 | $1.49 \times 10^{-2}$ |
| R2-FT2 | 4.3 | 2.45 | 2.43 | $1.98 \times 10^{-2}$ |
| R3-FT1 | 2.4 | 1.80 | 1.79 | $1.58 \times 10^{-2}$ |
| R3-FT2 | – | 2.76 | 2.73 | $2.34 \times 10^{-2}$ |
| R3-FT3 | – | 3.50 | 3.47 | $2.71 \times 10^{-2}$ |
| R3-FT4 | 3.2 | 6.81 | 6.78 | $2.89 \times 10^{-2}$ |

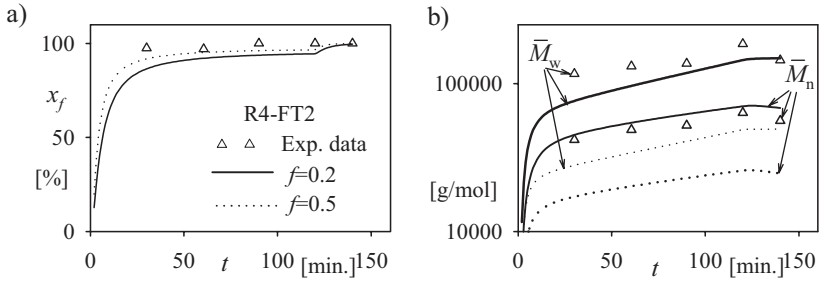


*Figure 8.* Semibatch experiment R4-FT2. Effect of changes in the initiation efficiency, $f$, on (a) fractional conversion, $x_f$; (b) number- and weight-average molar masses ($\overline{M}_n$ and $\overline{M}_w$).

branches around 200-fold over long branches (in number). However, long branches have an important effect on the polymer structure, and they must be taken into account to adequately fit the experimental $\overline{M}_w$ data. The simulation results also show that both short and long branches increase with the [KPS] and FT, as experimentally observed for the total BD.

Under the assumptions considered in this work, the model was able to adequately predict the whole experimental data evolution with a unique set of parameters. However, some of the adjusted kinetic constants could probably change if absolute (instead of pullulans-based) molar masses were employed.

It is generally accepted that: (i) different molar masses in PAA lead to large differences in the viscosity of the polymerization media; and (ii) the viscosity can govern the reactions between long-chain macromolecules and radicals, which can be diffusion controlled. For these reasons, chain length dependent rate coefficients such as $k_{tc}$ and $k_{fp}$,[21,22] would probably lead to a better fit of the experimental data. Nevertheless, it was preferred a model as simple as possible but yet satisfactory.

As previously mentioned, the average molar masses in the R4-FT2 experiment were not further reduced with respect to R3-FT2, even when [KPS] was doubled. This could be justified by a reduction in the initiation efficiency at high [KPS] (due to bimolecular termination of sulfate radicals). Figure 8 compares experimental data with simulation results for R4-FT2, at two different initiation efficiencies (the adopted $f = 0.5$ for reaction R1-, R2-, and R3-; and the adjusted $f = 0.2$ for experiment R4-FT2). Clearly, the reduction of $f$ at high [KPS] (and low [AA]) could explain the experimental evolution of the average molar masses observed for R4-FT2.

## Conclusion

The aqueous solution polymerization of non-ionized AA at 60 °C was investigated with the objective of producing PAA of controlled average molar masses, in a process operating under safe isothermal conditions, and reaching complete AA conversion. The proposed semibatch policy proved to be robust and effective for producing PAA with intermediate $\overline{M}_n$ ($1 \times 10^4$–$2 \times 10^5$ g · mol$^{-1}$), by adequately selecting the [KPS] and the AA FT. This approach could be of interest in industrial applications involving large reaction volumes.

Higher [KPS] and AA FT contribute to a meaningful reduction in the $\overline{M}_n$ of the produced PAA. However, increases in the PAA polydispersity were observed at the lowest AA feed rates and large [KPS]. As experimentally observed by NMR, the BD is augmented when increasing either [KPS] or AA FT.

A simple mathematical model that only included six kinetic parameters was able to adequately predict the tendency observed in the main reaction variables, i.e.: conversion, average molar masses, polydispersities, and BDs. According to the model results, the observed BD was mainly due to short branches from backbiting reactions. Thus, a low number of long branches was produced (from transfer to the polymer), that were responsible of the polydispersity increase observed at both large FT and large [KPS]. Finally, $^{13}$C NMR analyses confirmed the adopted kinetic mechanism.

## Mathematical Model for the AA Aqueous-Solution Polymerization

From the kinetic considerations and hypothesis previously described in the Kinetics and Mathematical Model section, the following balances can be written:

$$\frac{dN_{AA}}{dt} = F_{AA} - R_p V$$

$$\frac{dN_{KPS}}{dt} = -k_d\,[KPS]\,V$$

$$\frac{dV}{dt} = F_w v_w + F_{AA} v_{AA}$$

$$\frac{d\,(Q_0 V)}{dt} = \frac{\beta}{2} R_p V$$

$$\frac{d(Q_1 V)}{dt} = R_p V$$

$$\frac{d\,(Q_2 V)}{dt} = \left\{1 + 2\left(\frac{1 + C_{fp}Q_2/[AA]}{\beta + C_{fp}Q_1/[AA]}\right) + \beta\left(\frac{1 + C_{fp}Q_2/[AA]}{\beta + C_{fp}Q_1/[AA]}\right)^2\right\} R_p V$$

$$\frac{d(BD_s Q_1 V)}{dt} = k_{bb}\left[R^{\bullet}_{sec}\right] V$$

$$\frac{d(BD_l Q_1 V)}{dt} = k_{fp}\left[R^{\bullet}_{sec}\right] Q_1 V$$

with

$$[i] = \frac{N_i}{V}; \quad (i = AA, KPS)$$

$$R_p = \left(k_{p,sec}[R^{\bullet}_{sec}] + k_{p,tert}[R^{\bullet}_{tert}]\,[AA]\right)$$

$$\beta = \frac{k_{tc}[R^{\bullet}]^2}{R_p}$$

where $N_{AA}$ and $N_{KPS}$ are the moles of AA and KPS, respectively; $F_{AA}$ and $F_w$ are the molar AA and water feed rates; $V$ is the total reaction volume; $v_{AA}$ and $v_w$ are the molar volumes of AA and water at the reaction temperature; $Q_0$, $Q_1$, and $Q_2$ are the first three moments of the number chain-length distribution, $[i]$ is the molar concentration of the $i$ specie; and $BD_s$ and $BD_l$ are the BDs due to short and long branches, respectively.

The radical concentrations $[R^{\bullet}]$, $\left[R^{\bullet}_{sec}\right]$, and $\left[R^{\bullet}_{tert}\right]$ are calculated according to the following equations:

$$[R^{\bullet}] = \sqrt{\frac{f\ k_d[KPS]}{k_{tc}}}$$

$$\left[R^{\bullet}_{tert}\right] = \frac{k_{fp}\, Q_1 \left[R^{\bullet}_{sec}\right] + k_{bb}\left[R^{\bullet}_{sec}\right]}{k_{p,tert}\,[AA]}$$

$$\left[R^{\bullet}_{sec}\right] = [R^{\bullet}] - \left[R^{\bullet}_{tert}\right]$$

Fractional ($x_f$) and total ($x$) conversions are estimated by:

$$x_f(t) = \frac{\int_0^t F_{AA}\,dt - N_{AA}(t)}{\int_0^t F_{AA}\,dt}$$

$$x(t) = \frac{\int_0^{FT} F_{AA}\,dt - N_{AA}(t)}{\int_0^{FT} F_{AA}\,dt}$$

Finally, the average molar masses and the total BD are calculated from:

$$\overline{M}_n = M_{AA}\frac{Q_1}{Q_0}$$

$$\overline{M}_w = M_{AA}\frac{Q_2}{Q_1}$$

$$BD = BD_l + BD_s$$

where $M_{AA}$ represents the molar mass of AA.

Acknowledgements: We are grateful to Kimiker S. R. L., ANPCyT, and CONICET (Argentina) for the financial support of this work. We also thank Eng. Alberto Ardissone from Kimiker S. R. L. G. Caceres acknowledges the scholarship from the Panama government.

Received: December 23, 2010; Revised: March 3, 2011; Published online: April 12, 2011; DOI: 10.1002/mren.201000059

Keywords: control of molar masses; molar mass distribution; polyacrylic acid; radical polymerization; semibatch operation

[1] H. F. Mark, N. G. Gaylord, N. M. Bikales, *Encyclopedia of Polymer Science and Technology. Plastics, Resins, Rubbers, Fibers*, John Wiley & Sons, Inc, New York **1964**, Vol. 1, p. 197.
[2] B. Elvers, S. Hawkins, G. Schulz, *Ullmann's Encyclopedia of Industrial Chemistry*, 5th edition, VCH Publishers, Inc., New York **1992**, Vol. A21, p. 143.
[3] H. L. Greenwald, L. S. Luskin, *Handbook of water-soluble Gums and Resins*, R. L. Davidson, Ed., McGraw-Hill, New York **1980**.
[4] T. Spychaj, *Prog. Org. Coat.* **1989**, *17*, 71.
[5] H. Omidian, M. J. Zohuriaan-Mer, H. Bouhendi, *Int. J. Polym. Mater.* **2003**, *52*, 307.
[6] G. Bokias, A. Durand, D. Hourdet, *Macromol. Chem. Phys.* **1998**, *199*, 1387.
[7] H. Omidian, S. A. Hashemi, P. G. Sammes, I. G. Meldrum, *Polymer* **1998**, *39*, 3459.
[8] K. S. Anseth, R. A. Scott, N. A. Peppas, *Macromolecules* **1996**, *29*, 8308.
[9] H. Çatalgil-Giz, A. M. Giz, A. Alb, W. F. Reed, *J. Appl. Polym. Sci.* **2004**, *91*, 1352.
[10] I. Lacik, S. Beuermann, M. Buback, *Macromolecules* **2003**, *36*, 9355.
[11] M. Buback, P. Hesse, I. Lacik, *Maromol. Rapid Comm.* **2007**, *28*, 2049.
[12] M. Buback, P. Hesse, R. A. Hutchinson, P. Kasák, I. Lacík, M. Stach, I. Utz, *Ind. Eng. Chem. Res.*, **2008**, *47*, 8197.
[13] S. Beurmann, M. Buback, P. Hesse, R. A. Hutchinson, S. Kukučková, I. Lacík, *Macromolecules.* **2008**, *41*, 3513.
[14] M. D. Zammit, T. P. Davis, K. G. Suddaby, *Polymer* **1998**, *39*, 5789.
[15] C. Braunshier, C. Hametner, *QSAR Comb. Sci.* **2007**, *8*, 908.
[16] M. D. Goodner, C. N. Bowman, *Macromolecules* **1999**, *32*, 6552.
[17] C. Plessis, G. Arzamendi, J. R. Leiza, H. A. S. Schoonbrood, D. Charnot, J. M. Asua, *Macromolecules* **2000**, *33*, 4.
[18] R. Li, J. F. Schork, *Ind. Eng. Chem. Res.* **2006**, *45*, 3001.
[19] R. A. Scott, N. A. Peppas, *AIChE J.* **1997**, *43*, 135.
[20] S. S. Cutie, P. B. Smith, D. E. Henton, T. L. Staples, C. Powell, *J. Polym. Sci.: Part B: Polym. Phys.* **1997**, *35*, 2029.
[21] G. B. Smith, G. T. Russell, M. Yin, J. P. A. Heuts, *Eur. Polym. J.* **2005**, *41*, 225.
[22] R. J. Minari, V. I. Rodriguez, D. A. Estenoz, J. R. Vega, G. R. Meira, L. M. Gugliotta, *J. App. Polym. Sci.* **2010**, *116*, 590.